

# Machine Learning Calabi-Yau Three-Folds, Four-Folds, and Five-Folds

Kaniba Mady Keita<sup>a,b\*</sup> and Younouss Hamèye Dicko<sup>b,c</sup>

*a Centre de Calcul de Modélisation et de Simulation: CCMS*

*Department of Physics, Faculty of Sciences and Techniques, University of Sciences, Techniques and Technologies of Bamako, FST-USTTB, BP:E3206, Mali.*

*b Centre de Recherche en Physique Quantique et de ses Applications: CRPQA, Bamako, Mali.*

*c Institut de Consultation et d'Expertise en Education: ICE, Bamako, Mali.*

March 4, 2025

## Abstract

In this manuscript, we demonstrate, by using several regression techniques, that one can machine learn the other independent Hodge numbers of complete intersection Calabi-Yau four-folds and five-folds in terms of  $h^{1,1}$  and  $h^{2,1}$ . Consequently, we combine the Hodge numbers  $h^{1,1}$  and  $h^{2,1}$  from the complete intersection of Calabi-Yau three-folds, four-folds, and five-folds into a single dataset. We then implemented various classification algorithms on this dataset. For example, the accuracy of the Gaussian process and the naive Bayes classifications are all 100% when a binary classification of three-folds and four-folds is performed. With the Support Vector Machine (SVM) algorithm plots, a special corner is detected in the Calabi-Yau three-folds landscape (characterized by  $17 \leq h^{1,1} \leq 30$  and  $20 \leq h^{2,1} \leq 40$ ) when multiclass classification is performed. Furthermore, the best accuracy, 0.996459, in classifying Calabi-Yau three-folds, four-folds, and five-folds, is obtained with the naive Bayes classification.

---

\*E-mail: madyfalaye@gmail.com, kanibamady.keita@usttb.edu.ml

# 1 Introduction

Conformally Calabi-Yau manifolds are very useful in the field of string theory compactification [1–4]. For instance, nontrivial superconformal field theories are obtained upon compactifying various string theories on a Calabi-Yau Four-folds [5]. In addition, mirror symmetry alternated one of the Higgs branches with the Coulomb branch when the M-theory is compactified on the Calabi-Yau mirror four-folds [6]. Furthermore, the Kähler and complex structure moduli of the Calabi-Yau five-folds lived in different supermultiplets as a result of M-theory compactification in Calabi-Yau five-folds [7]. It should be stressed that these results, amongst others from string theory probes, gave new impetus to the construction of these Calabi-Yau manifolds [8–11]. Consequently, the number of possible Calabi-Yau manifolds that are complete intersections in products of projective spaces has been worked out. The complete intersection of Calabi-Yau is hereafter denoted by CICY.

There are 7890 Calabi-Yau three-folds and the list of these manifolds is available in [12]. However, this number drastically reduces to 266 as far as distinct Hodge numbers are considered. The number of complete intersections of Calabi-Yau four-folds is found to be 921497 and is available in ref.[13]. The number of distinct Hodge numbers for this list of CICY4 is 4418. For the Calabi-Yau five-folds, we consider the 27068 spaces obtained by the authors of ref.[14]. These authors calculated the cohomological data for 12433 (53.7%) of these manifolds. The data set obtained contains 2375 different Hodge numbers in its Hodge diamond. We use these 2375 different Hodge numbers (provided in the link of ref.[14]) in the present manuscript. In the classification algorithms, we exclusively consider these distinct Hodge numbers (266 for CICY3, 4418 for CICY4, and 2375 for CICY5). The data set is then subjected to various machine learning classification techniques.

Application of machine learning (ML) techniques to Calabi-Yau manifolds have recently been seriously investigated [15–30]. Throughout these probes, tangible pieces of evidence have been found, and aspects of CICY are machine-learnable. Much of these efforts used classifications and regression algorithms from supervised machine learning. The indicators judging the performance of these techniques have shown perfect learning so far. One of these metrics is the percentage of the target variable that is correctly predicted by the models: This metric is usually known as a  $R^2$  score for regressions. Another core metric for classification is the so-called accuracy and represents the ratio of the number correctly predicted by a model to the total number of the validation dataset <sup>1</sup>. In our previous article [31], we applied various regression algorithms to learn the Hodge number  $h^{2,1}$  in terms of  $h^{1,1}$  for CICY3. Here, we first adopt this approach to machine learning Hodge numbers  $h^{3,1}$  in terms of  $h^{2,1}$  and  $h^{1,1}$  for CICY4. The performance of these supervised learning suggests the generalization of regression to reduce the number of Hodge numbers for a given CICY. Consequently, we arrange the Hodge numbers  $h^{2,1}$  and  $h^{1,1}$  of CICY3, CICY4, and CICY5 in a single data frame. We then subject this data set to classification tasks such as Gaussian Process Regression (gausspr) [34], Naive Bayes[32, 33], Support Vector Classifier (SVM) [35–37], the random forest (RF) [38, 39], logistic regression [40], linear discriminant analysis (Lda) [41], recursive partitioning (rpart) [42], and finally k-Nearest Neighbor (Knn) [43]. The results reveal that these algorithms perform well in

---

<sup>1</sup>Very simple explanation of how to compute this accuracy and various statistical measures are given in [27].

classifying CICY3, CICY4, and CICY5.

The remainder of this manuscript is sectioned as follows. In section 2, we give an exploratory data analysis (EDA) of CICY3, CICY4, and CICY5. This EDA concerns the skewness [44] of the different Hodge numbers for the given CICY and the plot of some of these Hodge numbers. This is necessary since the class imbalance problem in deep learning is a troublesome situation [45]. In section 3, we apply various regression algorithms to learn  $h^{3,1}$  in terms of  $h^{1,1}$  and  $h^{2,1}$  for the reduced CICY4 dataset (4418). This is a continuation of our previous article [31] on CICY4. The results of these regressions demonstrate that CICY3, CICY4, and CICY5 can be classified using  $h^{1,1}$  and  $h^{2,1}$  as input of the algorithms. In section 4, we perform this classification task. We begin with the classification of CICY3 and CICY4 using the aforementioned algorithms. This binary classification is essential to see the connectedness of CICY. Then the classification of CICY3, CICY4, and CICY5 is followed. In section 5, we draw some conclusions and possible future directions for our findings.

## 2 Skewness analysis of CICY Three, Four and Five-folds

We begin this section by performing the skewness analysis of the data set of CICY3, CICY4, and CICY5. The skewness of the data set was shown to not alter the precision of machine learning classifications [46]. However, its relationship with the class imbalance problem in deep learning forces us to look at it. Let us start this overview by giving some basic information about any CICY.

Any CICY  $\mathbb{X}$  of complex dimension  $n$  is characterized by a *Configuration Matrix*  $\mathbb{C}$  given by.

$$\mathbb{C} = \begin{bmatrix} \mathbb{P}^{n_1} & \parallel & q_1^1 & \cdots & q_K^1 \\ \mathbb{P}^{n_2} & \parallel & q_1^2 & \cdots & q_K^2 \\ \vdots & & \vdots & \ddots & \vdots \\ \mathbb{P}^{n_m} & \parallel & q_1^m & \cdots & q_K^m \end{bmatrix} = \begin{bmatrix} n_1 & \parallel & q_1^1 & \cdots & q_K^1 \\ n_2 & \parallel & q_1^2 & \cdots & q_K^2 \\ \vdots & & \vdots & \ddots & \vdots \\ n_m & \parallel & q_1^m & \cdots & q_K^m \end{bmatrix}, \quad q_a^r \in \mathbb{Z}_{\geq 0}. \quad (1)$$

Where  $\mathbb{X}$  is a complete intersection of transverse hypersurfaces (homogeneous holomorphic polynomials)  $\mathbb{X}_1, \mathbb{X}_2, \dots, \mathbb{X}_K$  in  $\mathbb{P}^n$  having homogeneous degrees  $q_1^a, q_2^a, \dots, q_K^a$  concerning  $\mathbb{P}^{n_a}$ . The degree of the defining polynomials and the other parameters in the *Configuration Matrix*  $\mathbb{C}$  satisfy the following relationships.

$$\sum_{r=1}^m n_r = n + K, \quad \sum_{\alpha=1}^K q_\alpha^r = n_r + 1, \quad r = 1, \dots, m. \quad (2)$$

For a given CICY, one can work out the dimension of the Dolbeault cohomology group  $H^{p,q}$  which is called the Hodge number  $h^{p,q^2}$ . These Hodge numbers count the numbers of harmonic  $(p, q)$  forms in  $\mathbb{X}$ . The Euler characteristic of  $\mathbb{X}$  is then given in terms of them by the formula.

$$\chi = \sum_{p,q} (-1)^{p+q} h^{p,q} \quad (3)$$

---

<sup>2</sup>We have  $h^{p,q} = h^{n-p,n-q}$  and  $h^{p,q} = h^{q,p}$

This Euler characteristic determines the number  $N$  of generation in the non compact spacetime by the formula  $N = |\chi|/2$ . The quotient of  $\mathbb{X}$  by some of its freely acting groups yields a very small number of generation [47–49].

The holomorphic top form,  $(n, 0)$ -form, of any CICY is  $h^{n,0} = 1$  and simply connectedness (as for most if not all of the CICY) of  $\mathbb{X}$  implies that  $h^{1,0} = 0$ . Using these restrictions, one finds that the Hodge numbers form a diamond called the Hodge diamond, where the corners are fixed. The independent elements of this Hodge diamond can be skewed. The skewness measures the degree of asymmetry of a given distribution and it is related to the class imbalance problem. The generic formula for the skewness for a given Hodge number  $h^{p,q}$  in any CICY, is given by:

$$Skewness = \frac{\sum_{k=1}^N (h_k^{p,q} - \bar{h}^{p,q})^3}{(N-1)\sigma^3} \quad (4)$$

where,  $\bar{h}^{p,q}$  is the mean of  $h^{p,q}$ ;  $h_k^{p,q}$  is the  $k$ th value of  $h^{p,q}$ ;  $N$  represents the number of CICY which is the number of  $h^{p,q}$ ; and finally  $\sigma$  stands for the standard deviation of  $h^{p,q}$ . In the following plots and what to follow, the Hodge numbers  $h^{p,q}$  are denoted by  $Hpq$ .

## 2.1 Skewness of the Hodge numbers CICY3

Using the facts for CICY outlined in the last section, one observes that CICY3 has only two unspecified Hodge numbers  $h^{1,1}$  and  $h^{2,1}$ . The Euler number is given by the formula  $\chi = 2(h^{1,1} - h^{2,1})$ . The skewness of the Hodges numbers is given in Figure 1.

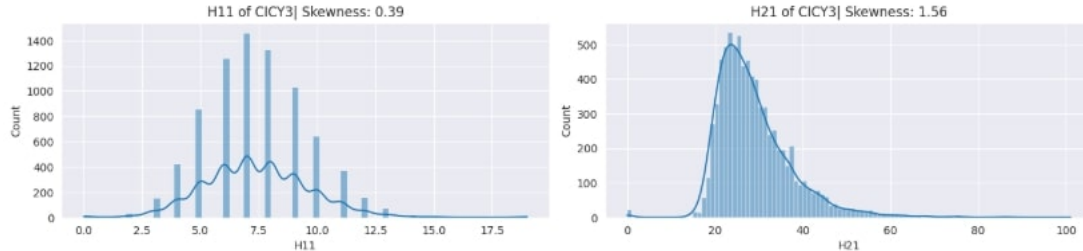


Figure 1: Skewness of the Hodge numbers for CICY3.

The plot of  $h^{2,1}$  as a function of  $h^{1,1}$  is depicted in Figure 2.

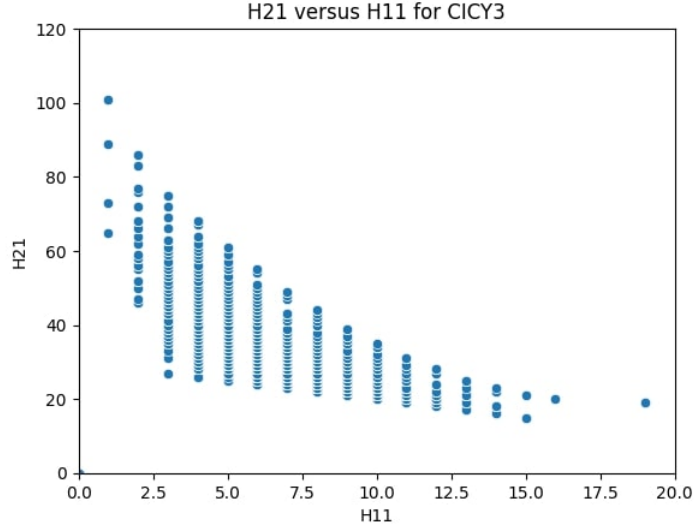


Figure 2:  $h^{2,1}$  as function of  $h^{1,1}$  for CICY3.

## 2.2 Skewness of the Hodge numbers for CICY4

The Hodge diamond of CICY4 has three independent Hodge numbers  $h^{1,1}$ ,  $h^{1,3}$ , and  $h^{1,2}$  due to the existence of an interesting linear relation [50].

$$h^{2,2} = 2(22 + 2h^{1,3} + 2h^{1,1} - h^{1,2}) \quad (5)$$

Consequently, we simply machine learn  $h^{1,3}$  in terms of  $h^{1,1}$  and  $h^{1,2}$  with various regressions techniques in section 3. The skewness of the Hodge numbers for CICY4 is presented in Figure 3.

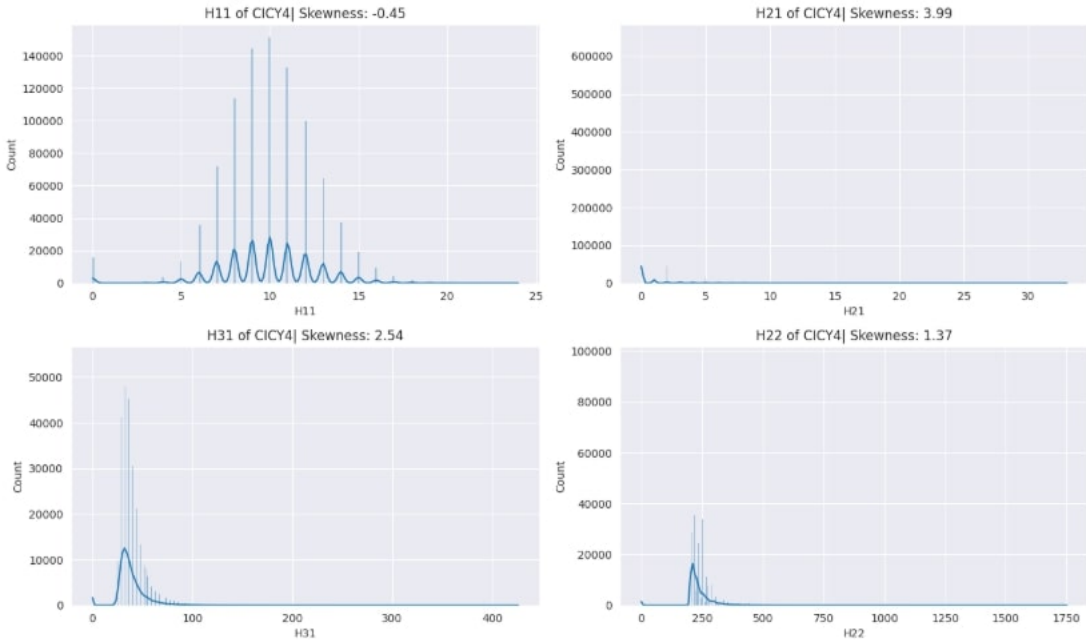
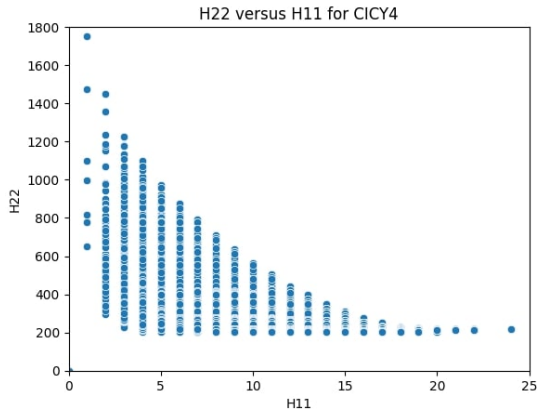


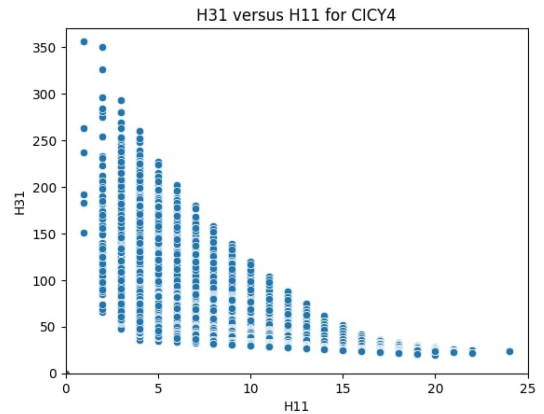
Figure 3: Skewness of the Hodge numbers of CICY4.

The plots of the other Hodge numbers can also be seen against  $h^{1,1}$  and  $h^{2,1}$  for CICY4.

These graphs illustrate the challenge facing the application of machine learning algorithms to the CICY4 dataset.

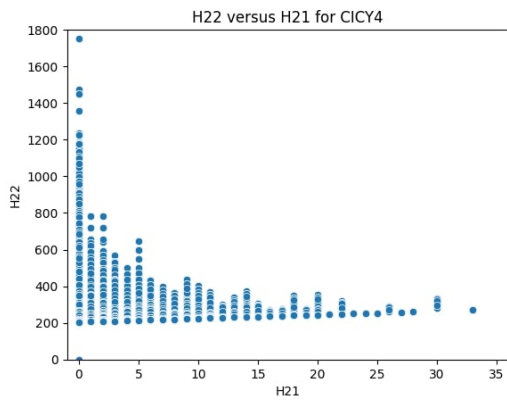


(a) H22 versus H11 for CICY4.

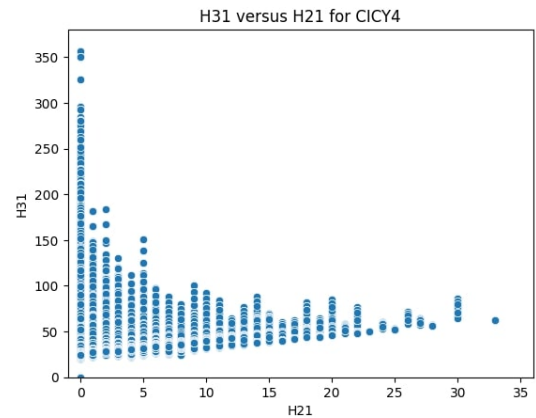


(b) H31 versus H11 for CICY4.

Figure 4: The plot of the other Hodge numbers versus H11 for CICY4.



(a) H22 versus H21 for CICY4.



(b) H31 versus H21 for CICY4.

Figure 5: The plot of the other Hodge numbers versus H21 for CICY4.

### 2.3 Skewness of the Hodge numbers for CICY5

The number of CICY5 is yet to be determined. However, the data set of ref.[14] deserves consideration. In CICY5, the Calabi-Yau condition yields  $h^{0,0} = h^{5,5} = 1$  and  $h^{1,0} = h^{0,1} = h^{4,5} = h^{5,4} = 0$ . The symmetry and duality of  $h^{p,q}$  set the unspecified Hodge numbers to be  $h^{1,1}$ ,  $h^{2,1}$ ,  $h^{3,1}$ ,  $h^{4,1}$ ,  $h^{2,2}$  and  $h^{3,2}$ . The skewness of these Hodge numbers for the dataset of CICY5 in [14] is shown in Figure 6.

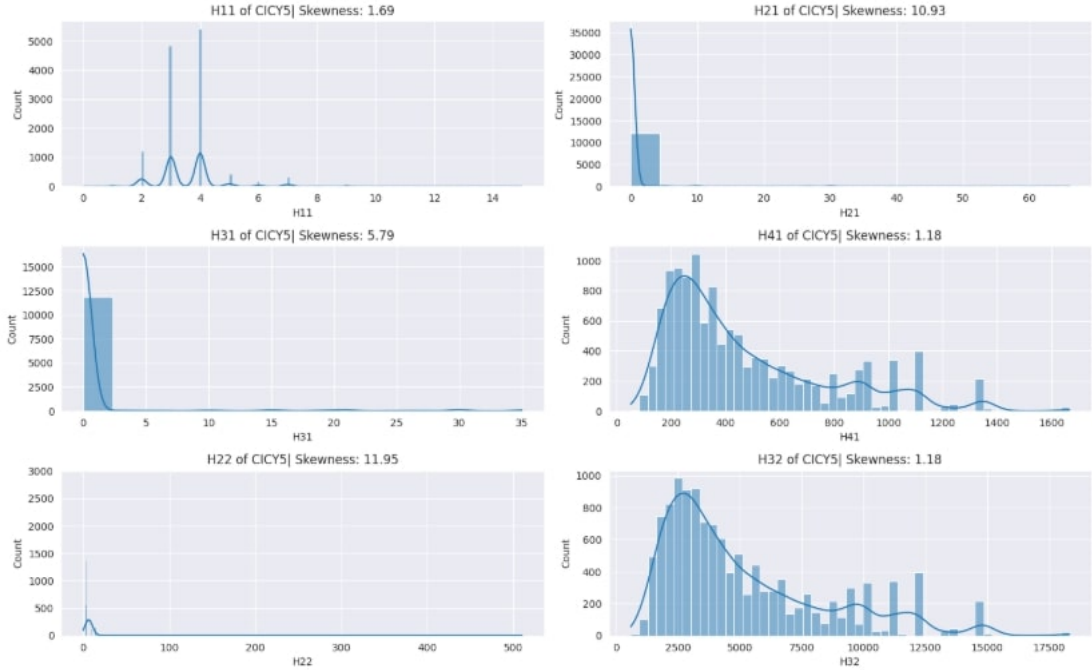


Figure 6: Skewness of the Hodge numbers for CICY5.

### 3 Learning $\hat{h}^{3,1} = f(h^{1,1}, h^{2,1})$ for the reduced CICY4 dataset

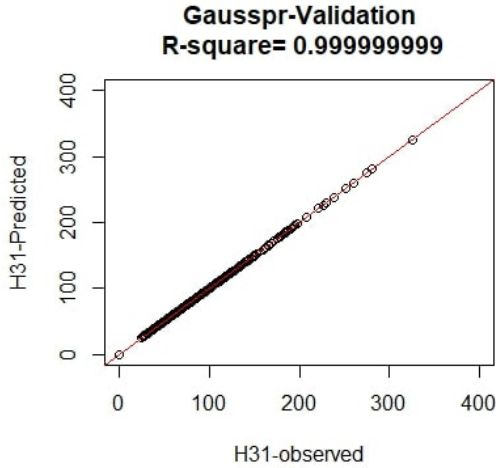
Before the classification tasks, we want to machine learn, if possible, the Hodge number  $h^{3,1}$  by taking as input the models  $h^{1,1}$  and  $h^{2,1}$ . To do so, we search for a hypothetical function  $f$  that schematizes this relationship.

The different regression techniques are trained with (80%) of the reduced 4418 data set of CICY4. The remaining (20%) are used for validating the models. The parameters used to judge the performance of the models are the **root mean square error (RMSE)** and the **Pearson correlation coefficient ( $R^2$ )**. The hyperparameters of the models are specified in [31]. The results of these machine learning approaches are given in Table 1.

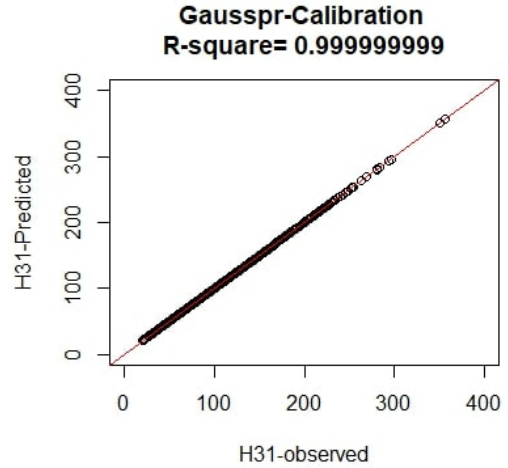
Table 1: Statistical measures for models applied to the 4418 of CICY4.

Regression	Validation		Calibration	
	$R^2$	RMSE	$R^2$	RMSE
gausspr	0.999999999	0.00207779	0.999999999	0.002105201
KSVM	0.9990968	2.510213	0.9990771	2.466058
RF	0.9969507	2.190028	0.9986549	1.555032
Xgboost	0.6094061	27.90818	0.5917905	25.56546

These results reveal that the Hodge number  $h^{3,1}$  of the reduced 4418 of CICY4 is easily learnable in terms of  $h^{1,1}$  and  $h^{2,1}$  by ML. In particular, Gaussian process regression is suitable in this dataset. The prediction of this algorithm against the true values is plotted in Figure 7.



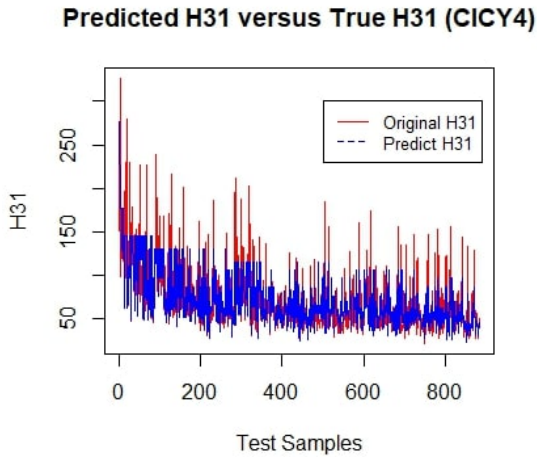
(a) gausspr for the validation set.



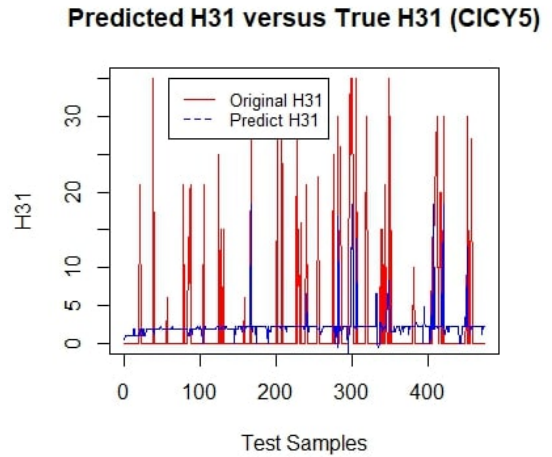
(b) Gausspr for the Calibration set.

Figure 7: The predictions from Gausspr for the reduced 4418 of CICY4.

The poorest performance is obtained with extreme gradient boost and its plots are shown in Figure 8



(a) Extreme gradient boost for CICY4.



(b) Extreme gradient boost for CICY5.

Figure 8: The plot of the Extreme gradient boost for CICY4 and CICY5.

As for the CICY5 dataset, a similar investigation can be performed in learning the others Hodge number in terms of  $h^{1,1}$  and  $h^{2,1}$  of the 2375 manifolds of CICY5. For example, learning  $h^{3,1}$  in terms of  $h^{1,1}$  and  $h^{2,1}$  using Gaussian process regression yields ( $R^2 = 100\%$ ,  $RMSE = 0.0005671492$ ) for the validation set and ( $R^2 = 100\%$ ,  $RMSE = 0.0005492653$ ) for the training set. However, the extreme gradient boost performs poorly with CICY5 ( $R^2 = 20.26\%$ ,  $RMSE = 7.148835$ ) for the validation set. These calculations show that an interesting dataset can be formed with CICY3, CICY4, and CICY5.

Consequently, we now consider  $h^{1,1}$  and  $h^{2,1}$  of CICY3, CICY4, and CICY5 in carrying out our classification tasks.

## 4 Classification of CICY

The goal of this section is to classify CICY3, CICY4 and CICY5 by simply using the Hodge numbers  $h^{1,1}$  and  $h^{2,1}$ . The performance of the classification models are recorded in the so-called *Confusion Matrix*. For instance, for classification with  $N$  classes, this matrix has the generic form:

$$\text{Confusion Matrix} = \begin{bmatrix} C_{11} & C_{12} & \cdots & C_{1N} \\ C_{21} & C_{22} & \cdots & C_{2N} \\ \vdots & \vdots & \ddots & \vdots \\ C_{N1} & C_{N2} & \cdots & C_{NN} \end{bmatrix}$$

which can alternatively be rewritten as

$$\text{Confusion Matrix} = \begin{bmatrix} \text{True} \setminus \text{Predicted} & \text{Class 1} & \text{Class 2} & \cdots & \text{Class N} \\ \text{Class 1} & C_{11} & C_{12} & \cdots & C_{1N} \\ \text{Class 2} & C_{21} & C_{22} & \cdots & C_{2N} \\ \vdots & \vdots & \vdots & \ddots & \vdots \\ \text{Class N} & C_{N1} & C_{N2} & \cdots & C_{NN} \end{bmatrix}$$

where  $C_{ii}$  represents the correct predictions fro class  $i$ ; whereas,  $C_{ij}(i \neq j)$  is the number of elements from class  $i$  misclassified as elements from class  $j$ .

To judge the classification models, we look at the **accuracy** and at **F1-Score** (for binary classification) or **F1-Score** per class (for multiclass classification). These metrics are derived from *Confusion Matrix* [51, 52].

In order to compute **accuracy** and **F1-Score** (for class  $i$ ), few concepts need to be recalled.

- True Positive (TP): Correctly predicted positives (diagonal).
- False Positive (FP): Misclassified negatives (column-wise, excluding diagonal).
- False Negative (FN): Missed positives (rowwise, excluding diagonal).
- True Negative (TN): Correctly predicted negatives (all except the row / column of interest).

They are mathematically expressed as follows.

$$\begin{aligned} \text{True Positive (TP)} &= C_{ii} \\ \text{False Positive (FP)} &= \sum_j C_{ji}(i \neq j) \\ \text{False Negative (FN)} &= \sum_j C_{ij}(j \neq i) \\ \text{True Negative (TN)} &= \sum_j C_{jj}(j \neq i) \end{aligned} \tag{1}$$

The accuracy by definition is the sum of the diagonal elements (true positives for each class) divided by the total number of samples.

$$\begin{aligned}
\text{Accuracy} &= \frac{\text{Sum of the diagonal elements (true positives for each class)}}{\text{Total number of samples}} \\
&= \frac{\text{Number of Correct Predictions}}{\text{Total Number of Predictions}} \\
&= \frac{TP + TN}{TP + TN + FP + FN} = \frac{\sum_{i=1}^N c_{ii}}{\sum_{i=1}^N \sum_{j=1}^N c_{ij}}.
\end{aligned} \tag{2}$$

The **F1-Score** for the class  $i$  is then computed as follows:

$$\begin{aligned}
\text{Precision} &= \frac{TP}{TP + FP} = \frac{C_{ii}}{C_{ii} + \sum_j C_{ji}(i \neq j)} \\
\text{Recall} &= \frac{TP}{TP + FN} = \frac{C_{ii}}{C_{ii} + \sum_j C_{ij}(j \neq i)} \\
\text{F1 Score} &= \frac{2 \times \text{Precision} \times \text{Recall}}{\text{Precision} + \text{Recall}}
\end{aligned} \tag{3}$$

We are now in a position to classify CICY using  $h^{1,1}$  and  $h^{2,1}$  as input of our algorithms. We begin with the binary classification of CICY3 and CICY4.

#### 4.1 Binary Classification of CICY3 and CICY4

Binary classification can be considered as a warm-up exercise for multiclass classification. The *Confusion Matrix* for this classification and the aforementioned measures are given in Table 2 for the validation sets and Table 3 for the train set. One notices that Gaussian process and Naive Bayes classifications are similar and pretty excellent algorithms for accomplishing this task. Therefore, in our multiclass classification problem, we simply consider the naive Bayes classification approach. These tables show condensed pieces of information in the *Confusion Matrices*. The diagonal elements are the ones which have been correctly classified. The off diagonal elements represent the number of CICY misclassified by the model under consideration. As an illustration, in the validation sets, **one CICY3** is considered as CICY4 and **eight CICY4** are viewed as CICY3 by the Knn algorithm.

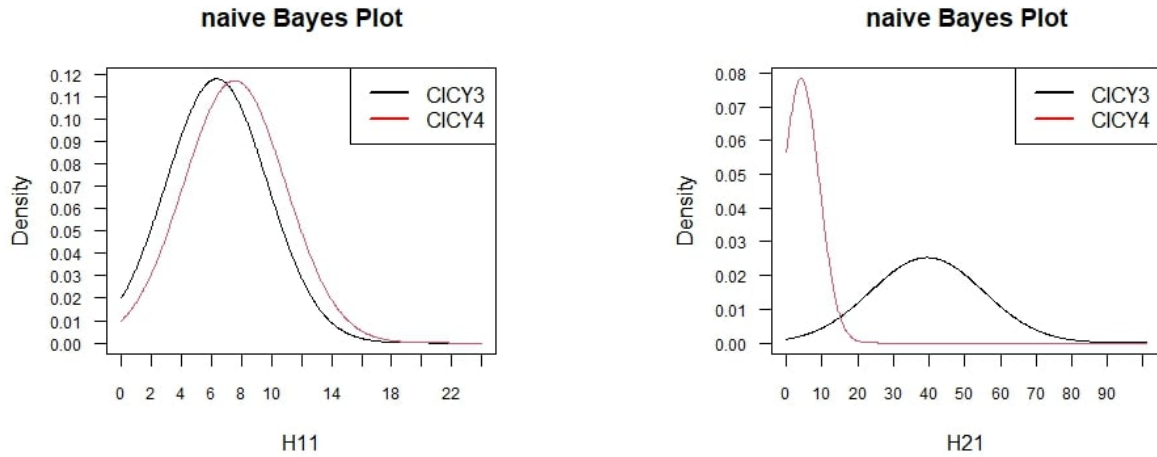
Table 2: Binary Classifications of CICY3& 4 Validation sets

Classification	Accuracy	F1-SCORE	Confusion Matrix		
			Class	CICY3	CICY4
Gausspr	1.00000000	1.00000	Class	CICY3	CICY4
			CICY3	<b>49</b>	0
			CICY4	0	<b>888</b>
Naive Bayes	1.00000000	1.00000	Class	CICY3	CICY4
			CICY3	<b>49</b>	0
			CICY4	0	<b>888</b>
Knn	0.9903949	0.9949	Class	CICY3	CICY4
			CICY3	<b>48</b>	1
			CICY4	8	<b>880</b>
Logistic	0.9882604	0.89109	Class	CICY3	CICY4
			CICY3	<b>45</b>	4
			CICY4	7	<b>881</b>
Rpart	0.9882604	0.87982	Class	CICY3	CICY4
			CICY3	<b>46</b>	3
			CICY4	8	<b>880</b>
Lda	0.9861259	0.86936	Class	CICY3	CICY4
			CICY3	<b>44</b>	5
			CICY4	8	<b>880</b>
svm	0.9861259	0.87129	Class	CICY3	CICY4
			CICY3	<b>44</b>	5
			CICY4	8	<b>880</b>

Table 3: Binary Classifications of CICY3&4 Training sets

Classification	Accuracy	F1-SCORE	Confusion Matrix		
			Class	CICY3	CICY4
Gausspr	1.00000000	1.00000	Class	CICY3	CICY4
			CICY3	<b>217</b>	0
			CICY4	0	<b>3530</b>
Naive Bayes	1.00000000	1.00000	Class	CICY3	CICY4
			CICY3	<b>217</b>	0
			CICY4	0	<b>3530</b>
Knn	0.9869229	0.9931	Class	CICY3	CICY4
			CICY3	<b>195</b>	22
			CICY4	27	<b>3503</b>
Rpart	0.9858554	0.87982	Class	CICY3	CICY4
			CICY3	<b>194</b>	23
			CICY4	30	<b>3500</b>
svm	0.9855885	0.87324	Class	CICY3	CICY4
			CICY3	<b>186</b>	31
			CICY4	23	<b>3507</b>
Logistic	0.9855885	0.87264	Class	CICY3	CICY4
			CICY3	<b>185</b>	22
			CICY4	22	<b>3508</b>
Lda	0.9853216	0.86936	Class	CICY3	CICY4
			CICY3	<b>183</b>	34
			CICY4	21	<b>3509</b>

These results show that CICY can be classified using the two Hodge numbers as input. The best models are the Gaussian process and naive Bayes classifications. In addition, Figure 9 shows the naive Bayes plot of the density for the two Hodge numbers of CICY3 and CICY4. These plots show the likelihood of the Hodge numbers for the given class.



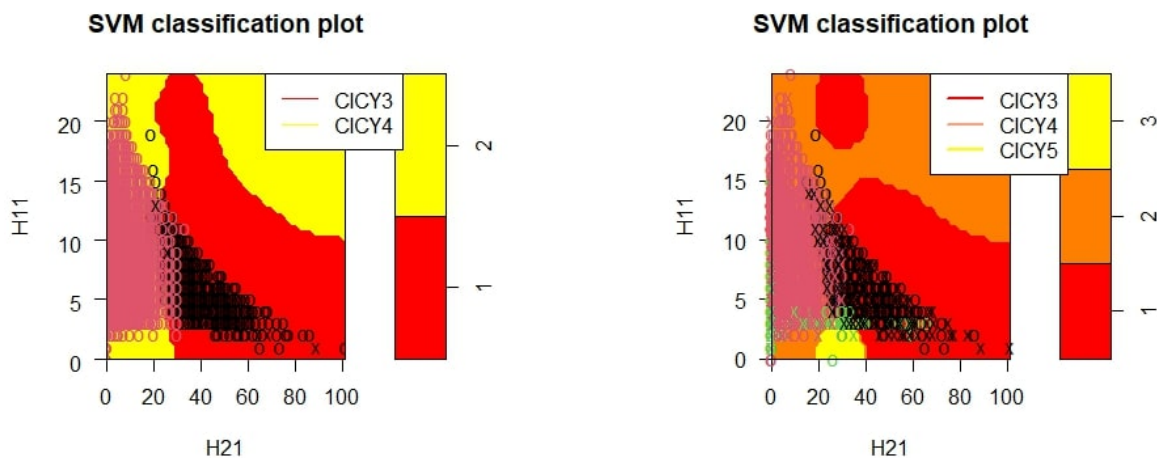
(a) Naive Bayes plot of H11.

(b) Naive Bayes plot of H21.

Figure 9: Naive Bayes plot of the Hodge numbers for CICY3 and CICY4.

In the naive Bayes graphs, there are no overlapping densities. This is very good since it indicates that the two Hodge numbers are discriminative for CICY3 and CICY4. It is visible that the densities are well separated. Hence,  $h^{1,1}$  and  $h^{2,1}$  are very useful to distinguish between CICY3 and CICY4.

Moreover, the graph for the decision boundary of the support vector machine 10a is useful. We observe the boundary separation of CICY3 and CICY4. We see that some of the CICY3 overlaps parts of CICY4.



(a) SVM plot of CICY3 and CICY4.

(b) SVM plot of the three CICYs.

Figure 10: SVM plot of the Data from SVM classification.

## 4.2 Multiclass Classification of CICY3, CICY4 and CICY5

With the successful learning classification of the last subsection, let us apply the algorithms in the process of recognizing CICY when  $h^{1,1}$  and  $h^{2,1}$  are the only available data. The performance of the models applied is surely affected due to the lack of missing values of CICY5. We therefore expected some of the CICY5 manifolds to be misclassified, which can lead to the misclassification of some of CICY3 and CICY4. This in principle should not drastically affect the overall outcomes. We obtain the following results Table 4 and Table 5 as performance outcomes in our classification tasks.

Table 4: Parameters for some Classifications Techniques (validation sets)

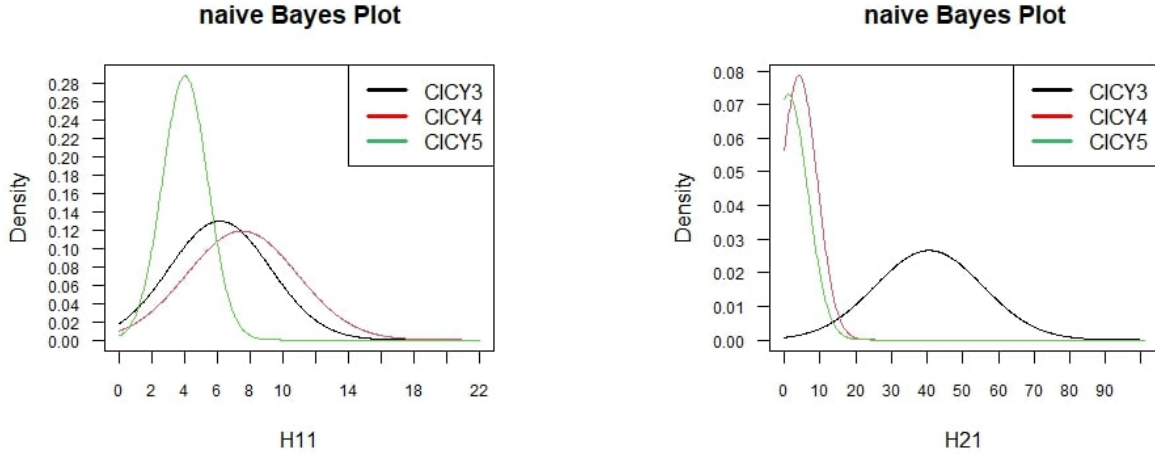
Classification	Accuracy	F1-SCORE			Confusion Matrix			
		CICY3	CICY4	CICY5	Class	CICY3	CICY4	CICY5
Naives Bayes	0.996459	0.97872	0.9988	0.9948	Class	CICY3	CICY4	CICY5
					CICY3	<b>69</b>	0	0
					CICY4	0	<b>861</b>	0
					CICY5	3	2	<b>477</b>
Ksvm	0.8675637	0.83077	0.8928	0.8282	CICY3	<b>54</b>	15	0
					CICY4	4	<b>766</b>	91
					CICY5	3	74	<b>405</b>
Rpart	0.861898	0.82857	0.8946	0.8031	CICY3	<b>58</b>	10	1
					CICY4	6	<b>794</b>	61
					CICY5	7	110	<b>365</b>
Svm	0.8611898	0.83077	0.8867	0.8214	CICY3	<b>54</b>	15	0
					CICY4	4	<b>755</b>	102
					CICY5	3	72	<b>407</b>
Lda	0.8328612	0.76336	0.8682	0.7788	CICY3	<b>50</b>	18	1
					CICY4	5	<b>751</b>	105
					CICY5	7	100	<b>375</b>

Table 5: Parameters for some Classifications Techniques (training sets)

Classification	Accuracy	F1-SCORE			Confusion Matrix			
		CICY3	CICY4	CICY5	Class	CICY3	CICY4	CICY5
Naives Bayes	0.998052	0.9728	1.0000	0.9971	Class	CICY3	CICY4	CICY5
					CICY3	<b>197</b>	0	0
					CICY4	0	<b>3557</b>	0
					CICY5	11	0	<b>1882</b>
Ksvm	0.8613423	0.86341	0.8899	0.8103	CICY3	<b>177</b>	17	3
					CICY4	23	<b>3100</b>	434
					CICY5	13	293	<b>1587</b>
Rpart	0.8563839	0.81069	0.8929	0.7895	CICY3	<b>182</b>	15	0
					CICY4	31	<b>3219</b>	307
					CICY5	39	419	<b>1435</b>
Svm	0.8484151	0.84264	0.8785	0.7970	CICY3	<b>166</b>	27	0
					CICY4	18	<b>3033</b>	506
					CICY5	13	288	<b>1592</b>
Lda	0.8284045	0.79439	0.8674	0.7610	CICY3	<b>170</b>	27	0
					CICY4	22	<b>3043</b>	492
					CICY5	39	389	<b>1465</b>

One observes that the naive Bayes algorithm is a very suitable model in our multiclass classification. The perfect learning is a positive result.

Finally, it is interesting to see the naive Bayes plots Figure 11 for our multiclass classification.



(a) Naive Bayes plots of H11.

(b) Naive Bayes plots of H21.

Figure 11: Naive Bayes plot of the Hodge numbers for CICY3, CICY4 and CICY5.

In these naive Bayes graphs, we witness overlapping densities for high values of  $h^{1,1}$  and for most of the values of  $h^{2,1}$ . A possible explanation is that a lot of Hodge numbers of CICY5 are still to be determined. It is observable that the densities are well separated for  $h^{1,1}$ .

The graph Figure 10b of the support vector machine in the multiclass classification shows that part of CICY3 are shadowed by CICY4 and CICY5. However, a corner in the Calabi-Yau three-folds landscape (characterized by  $17 \leq h^{1,1} \leq 30$  and  $20 \leq h^{2,1} \leq 40$ ) is observable from Figure 10b. It is also visible that CICY5 is masking both CICY3 and CICY4 in the region ( $0 \leq h^{1,1} \leq 4$  and  $20 \leq h^{2,1} \leq 40$ ) which is quiet surprising.

## 5 Conclusions

This manuscript addresses issues of Calabi-Yau manifolds classifications throughout the use of machine learning algorithms. Our investigations reveal that complete intersection Calabi-Yau three-folds, four-folds and five-folds can be classified by using techniques from supervised machine learning.

There are no overlapping densities in the plot of the naive Bayes binary classification of CICY3 and CICY4. Therefore, the two Hodge numbers are discriminative for CICY3 and CICY4. Additionally, the densities are well separated. In conclusion,  $h^{1,1}$  and  $h^{2,1}$  are very useful to distinguish between CICY3 and CICY4. However, an overlapping of the densities is observed in the classification of CICY3, CICY4 and CICY5. The window of CICY3 not masked by CICY4 and CICY5 needs further considerations.

## References

- [1] Andrew Strominger and Edward Witten, **New Manifolds for Superstring Compactification**. Commun. Math. Phys. **101**, 341-361 (1985).
- [2] P. Candelas, Gary T. Horowitz, A. Strominger, E. Witten; **Vacuum Configurations for Superstrings**, Nucl. Phys. B **258** (1985) 46-74.
- [3] Brian R. Greene, **String Theory on Calabi-Yau Manifolds**. *arXiv : hep - th/9702155*.
- [4] Mariana Graña **Flux compactifications in string theory: a comprehensive review**. Physics Reports, **423** (3):91-158, January 2006. ISSN 03701573. doi: 10.1016/j.physrep.2005.10.008.
- [5] S. Gukov, C. Vafa and E. Witten, **CFT'S from Calabi- Yau Four-Folds**. Nuclear Physics B **584** (2000) 69-108.
- [6] B.S. Acharya. **A mirror pair of Calabi-Yau four-folds in Type II string theory**. Nuclear Physics B **524** (1998) 283-294.
- [7] Alexander S Haupt, Andre Lukas, K. S. Stelle. **M-theory On Calabi-Yau Five-Folds**. JHEP **05** (2009) 069.
- [8] P. Candelas A.M. Dale C.A. Lutken, **Complete Intersection Calabi-Yau Manifolds**, Nucl.Phys. B **298** (1988) 493.
- [9] Anming He and Philip Candelas, **On the Number of Complete Intersection Calabi-Yau Manifolds**. Commun. Math. Phys. **135**, 193-199 (1990).
- [10] T. Hubsch, **Calabi-Yau Manifolds- Motivations and Constructions**, Commun. Math. Phys. **108**, 291-318 (1987).
- [11] Paul Green and Tristan Hubsch, **Calabi-Yau Manifolds as Complete Intersections in Products of Complex Projective Spaces**. Commun. Math. Phys. **109**, 99-108 (1987).
- [12] P.S. Green, T. H. Hubsch and C. A. Lutken, **All the Hodge numbers for all Calabi-Yau complete intersections**, Class.Quantum.Grav. **6** (1989) 105-124.**Data set of Complete Intersection of Calabi-Yau Three-foldsss**. [https : //www - thphys.physics.ox.ac.uk/projects/CalabiYau/cicylist/](https://www-thphys.physics.ox.ac.uk/projects/CalabiYau/cicylist/).
- [13] James Gray, Alexander S. Haupt, and Andre Lukas. **All Complete Intersection Calabi-Yau Four-Folds**. JHEP **07** (2013) 070. [https : //www - thphys.physics.ox.ac.uk/projects/CalabiYau/Cicy4folds/index.html](https://www-thphys.physics.ox.ac.uk/projects/CalabiYau/Cicy4folds/index.html).
- [14] R. Alawadhi, D. Angella, A. Leonardo, T. Schettini Gherardini. **Constructing and Machine Learning Calabi-Yau Five-folds**. Fortschr. Phys. **2023**, 2300262, arXiv:2310.15966 [hep-th].
- [15] Yang-Hui He, **The Calabi-Yau Landscape:from Geometry, to Physics, to Machine-Learning**, arxiv: 1812:02893.
- [16] Yang-Hui He, **Deep-Learning the Landscape**, arXiv:1706.02714.

- [17] Yang-Hui He, Zhi-Gang Yao, Shing-Tung Yau. **Distinguishing Calabi-Yau Topology using Machine Learning**. e-Print: 2408.05076 [math.AG].
- [18] Wei Cui, Xin Gao, and Juntao Wang, **Machine Learning on generalized Complete Intersection Calabi-Yau Manifolds**, arXiv:2209.10157.
- [19] Harold Erbin, and Riccardo Finotello, **Deep learning complete intersection Calabi-Yau manifolds**, [arXiv:2311.11847 [hep-th]].
- [20] Anthony Ashmore, Yang-Hui He, and Burt Ovrut, **Machine learning Calabi-Yau metrics**, Fortsch.Phys. **68** (2020) 9, 2000068.
- [21] D. Aggarwal, Y.-H. He, E. Heyes, E. Hirst, H. N. S. Earp, and T. S. R. Silva, **Machine-learning Sasakian and G2 topology on contact Calabi-Yau 7-manifolds**, arXiv:2310.03064 [math.DG].
- [22] D. S. Berman, Y.-H. He, and E. Hirst, **Machine learning Calabi-Yau hypersurfaces**, Phys.Rev. D 105 no. **6**, (2022) 066002, arXiv:2112.06350 [hep-th].
- [23] R. Alawadhi, D. Angella, A. Leonardo, T. Schettini Gherardini, **Constructing and Machine Learning Calabi-Yau Five-folds**, arXiv:2310.15966.
- [24] Rehan Deen, Yang-Hui He, Seung-Joo Lee, and Andre Lukas, **Machine learning string standard models**, Phys. Rev. D **105**, 046001 (2022).
- [25] Yang-Hui He and Andre Lukas, **Machine learning Calabi-Yau four-folds**, Phys.Lett.B **815** (2021) 136139.
- [26] F. Ruehle, **Data science applications to string theory**, Phys. Rep. **839** (2020) 1.
- [27] K. Bull, Y.H. He, V. Jejjala, and C. Mishra, **Machine learning CICY Three-foldssss**, Phys.Lett. B **785** (2018) 65–72, arXiv:1806.03121.
- [28] Kieran Bull, Yang-Hui He, Vishnu Jejjala, Challenger Mishra. **Getting CICY High**. Phys.Lett.B **795** (2019) 700-706. DOI: 10.1016/j.physletb.2019.06.067; e-Print: 1903.03113 [hep-th].
- [29] H. Erbin and R. Finotello, **Inception neural network for complete intersection Calabi-Yau 3-folds**, Mach. Learn.: Sci. Technol. 2021, **2**, 02LT03., arXiv:2007.13379.
- [30] Harold Erbin, Riccardo Finotello, Robin Schneider and Mohamed Tamaazousti, **Deep multi-task mining Calabi–Yau four-folds**, Mach. Learn.: Sci. Technol. 2022, **3** 015006.
- [31] Kaniba Mady Keita. **Machine learning complete intersection Calabi-Yau 3-folds**. Phys.Rev.D **110** (2024) 12, 126002. e-Print: 2404.11710 [hep-th].
- [32] Pedro Domingos & Michael Pazzani. **On the Optimality of the Simple Bayesian Classifier under Zero-One Loss**. Machine Learning, **29**, 103–130 (1997).
- [33] David J. Hand and Keming Yu. **Idiot’s Bayes: Not So Stupid after All?**. International Statistical Review / Revue Internationale de Statistique, Vol. 69, No. 3 (Dec., 2001), pp. 385-398.

- [34] C.K.I. Williams and D. Barber, **Bayesian classification with Gaussian processes**, IEEE Transaction on Pattern Analysis and Machine Intelligence, **20** (12): 1342-1351, 1998, DOI: 10.1109/34.735807.
- [35] V Vapnik, **The nature of Statistical learning theory**, Springer, New York (1995).
- [36] Corinna Cortes and Vlafmir Vapnik, **Support- Vector Networks**, Machine Learning, **20**, 273-297 (1995).
- [37] H. Drucker, C. J. Burges, L. Kaufman, A. Smola and V. Vapnik, **Support vector regression machines**, Advances in Neural Information Processing Systems **9** (NIPS 1996).
- [38] Leo Breiman, **Bagging predictors**. Machine Learning, **6** (2), 123-140, 1996
- [39] Leo Breiman, **Random Forests**, Machine Learning, **45**, 5-32, 2001.
- [40] B. Efron. **The efficiency of logistic regression compared to Normal Discriminant Analysis**. Journ. of the Amer. Statist. Assoc., **70**:892- 898, 1975.
- [41] D.L. Swets and J.J. Weng. **Using Discriminant Eigenfeatures for Image Retrieval**. IEEE Trans. Pattern Analysis and Machine Intelligence, vol. 18, no. 8, pp. 831-836, Aug. 1996.
- [42] Carolin Strobl, James Malley and Gerhard Tutz. **An Introduction to Recursive Partitioning: Rationale, Application and Characteristics of Classification and Regression Trees, Bagging and Random Forests**. Psychol Methods. 2009 Dec;14(4):323-48. doi : 10.1037/a0016973. PMID: 19968396; PMCID: PMC2927982.
- [43] T. Cover and P. Hart, **Nearest neighbor pattern classification**. IEEE Transactions on Information Theory, vol. 13, no. 1, pp. 21-27, January 1967, doi : 10.1109/TIT.1967.1053964.
- [44] Hippel, Paul von. **Skewness**. In: Lovric, M. (eds) International Encyclopedia of Statistical Science. Springer, Berlin, Heidelberg. DOI: 10.1007/978-3-642-04898-2\_25.
- [45] Ghosh, K., Bellinger, C., Corizzo, R. et al. **The class imbalance problem in deep learning**. Mach Learn **113**, 4845–4901 (2024). DOI: 10.1007/s10994-022-06268-8.
- [46] A Larasati, A M Hajji and Anik Dwiastuti, **The relationship between data skewness and accuracy of Artificial Neural Network predictive model**. A Larasati et al **2019 IOP Conf. Ser.: Mater. Sci. Eng.** 523 012070. DOI: 10.1088/1757-899X/523/1/012070.
- [47] P. Candelas and C.A. Lutken, **Complete Intersection Calabi-Yau Manifolds. 2. Three Generation Manifolds**, Nucl.Phys. B **306** (1988) 113.
- [48] P. Candelas, **Yukawa Couplings for a Three Generation Superstring Compactification**, Nucl. Phys. B **298** (1988) 357-368.
- [49] Rolf Schimmrigk, **A New Construction of a Three Generation Calabi-Yau Manifold**, Phys.Lett.B **193** (1987) 175.

- [50] Gray, J., Haupt, A.S. & Lukas, A. **Topological invariants and fibration structure of complete intersection Calabi-Yau four-folds**. J. High Energ. Phys. 2014, 93 (2014). [https://doi.org/10.1007/JHEP09\(2014\)093](https://doi.org/10.1007/JHEP09(2014)093).
- [51] Markoulidakis I, Rallis I, Georgoulas I, Kopsiaftis G, Doulamis A, Doulamis N. **Multiclass Confusion Matrix Reduction Method and Its Application on Net Promoter Score Classification Problem**. Technologies. 2021; 9(4):81. <https://doi.org/10.3390/technologies9040081>.
- [52] Andreas Theissler, Mark Thomas, Michael Burch, Felix Gerschner. **Confusion-Vis: Comparative evaluation and selection of multi-class classifiers based on confusion matrices**. Knowledge-Based Systems 247 (2022) 108651. <https://doi.org/10.1016/j.knosys.2022.108651>.